

The Role of Elastase in Corneal Epithelial Barrier Dysfunction Caused by *Pseudomonas aeruginosa* Exoproteins

Ye Li,¹ YingWei Wang,¹ ChunWei Li,² DePeng Zhao,³ QinYuan Hu,¹ Min Zhou,¹ Miao Du,¹ Jian Li,² and PengXia Wan¹

¹Department of Ophthalmology, The First Affiliated Hospital, Sun-Yat-sen University, Guangzhou, China

²Department of Otolaryngology, The First Affiliated Hospital, Sun-Yat-sen University, Guangzhou, China

³School of Pharmaceutical Sciences, Sun-Yat-sen University, Guangzhou, China

Correspondence: PengXia Wan, Department of Ophthalmology, The First Affiliated Hospital, Sun-Yat-sen University, N0.58, Zhongshan Second Road, Guangzhou 510080, China;

wanpengx@mail.sysu.edu.cn.

Jian Li, Department of Otolaryngology, The First Affiliated Hospital, Sun-Yat-sen University, N0.58, Zhongshan Second Road, Guangzhou 510080, China; lijian7@mail.sysu.edu.cn.

Received: January 18, 2021

Accepted: May 18, 2021

Published: July 7, 2021

Citation: Li Y, Wang Y, Li C, et al. The role of elastase in corneal epithelial barrier dysfunction caused by *Pseudomonas aeruginosa* exoproteins. *Invest Ophthalmol Vis Sci*. 2021;62(9):7. <https://doi.org/10.1167/iovs.62.9.7>

PURPOSE. To investigate the role of elastase in corneal epithelial barrier dysfunction caused by the exoproteins secreted by *Pseudomonas aeruginosa*.

METHODS. Exoproteins obtained from *Pseudomonas aeruginosa* culture supernatant were analyzed by shotgun proteomics approach. In vitro multilayered rabbit corneal epithelial barrier model prepared by air-liquid interface technique (CECs-ALI) were treated with 2 µg/ml exoproteins and/or 8 mM elastase inhibitor. Then the epithelial barrier function was evaluated by transepithelial electrical resistance (TEER) assay and tight junction proteins immunofluorescence. Cell viability and the apoptosis rate were examined by CCK8 assay and flow cytometry. TNF-α, IL-6, IL-8, and IL-1β levels were measured by ELISA. Mice cornea treated with exoproteins and/or elastase inhibitor were evaluated in vivo and in vitro.

RESULTS. Elastase (24.2%) is one of the major components of exoproteins. After 2 µg/ml exoproteins were applied to CECs-ALI for two hours, TEER decreased from 323.2 ± 2.7 to 104 ± 6.8 Ω/cm² ($P < 0.001$). The immunofluorescence results showed a distinct separation in tight junction and significant degradation of ZO-1 and occludin ($P < 0.05$). Elastase inhibitor (8 mM) alleviated the decrease in TEER value (234 ± 6.8 Ω/cm²) induced by exoproteins. Inhibition of elastase decreased the apoptosis rate of CECs treated with exoproteins from 30.2 ± 3.8% to 7.26 ± 1.3% and the levels of inflammatory factors ($P < 0.05$). Mice corneal epithelium defect could be induced by exoproteins and protected by elastase inhibitor.

CONCLUSIONS. Elastase plays a critical role in corneal epithelial barrier dysfunction caused by *Pseudomonas aeruginosa* exoproteins via damaging tight junctions. The inhibition of elastase could protect the corneal epithelial barrier via reducing virulence and inflammation.

Keywords: corneal epithelial barrier, elastase, *Pseudomonas aeruginosa*

Pseudomonas aeruginosa (*P. aeruginosa*) is an opportunistic bacterial pathogen causing serious infections of the airway, skin, or the cornea, particularly in patients with defects in the epithelial barrier.¹ Previous studies have shown that healthy cornea could resist *P. aeruginosa* infection because intact corneal epithelium provides a major barrier to bacterial pathogens.^{2,3} The adhesion and penetration of *P. aeruginosa* to corneal epithelium are earlier steps in the process of *P. aeruginosa* colonization. It is commonly thought that injured corneal epithelium provided a surface for *P. aeruginosa* to adhere and *P. aeruginosa* can penetrate the multilayered corneal epithelium or invade the corneal stroma through the wounded corneal areas.⁴ However, recent studies showed that subtle injury to the superficial epithelium could allow *P. aeruginosa* to adhere to the cornea, but not penetrate beyond the epithelial barrier, which implicates that defenses against these two

steps in corneal infection are separable.⁵ The success of *P. aeruginosa* invasion partly depends on the production of exoproteins.⁶ *P. aeruginosa* exoproteins include proteases, toxins, and pyocyanin that promote invasion by degrading host structural or immune proteins and enhancing the mucosal permeability in the early stage of infection.⁷ It indicates exoproteins are the main contributing factors in the early process of *P. aeruginosa* infection. Despite substantial evidence of the role of *P. aeruginosa* exoproteins in airway disease, inflammatory bowel disease, and atopic dermatitis,⁸ the effects of *P. aeruginosa* exoproteins on the corneal epithelial barrier function and the interaction between corneal epithelial cells and exoproteins remain unknown.

The fundamental treatment of *P. aeruginosa* keratitis is based on bactericidal antibiotic therapy to eliminate the bacteria, which cannot reverse the damage caused by

P. aeruginosa exoproteins. Even with aggressive antibiotic therapy, the infections can rapidly progress to corneal perforation, an event attributed to the bacterial proteases, the activation of matrix metalloproteinase, and a damaging immune response.⁹ Previous studies have confirmed the strong correlation between corneal virulence and proteases production. Adjunct therapies to limit the action of these proteases are promising tools to be explored, which can slow down the progression of *P. aeruginosa* keratitis and provide time for subsequent therapy to save the vision. The protease-related virulence of the *P. aeruginosa* exoproteins is mainly dependent on elastase as previously reported.¹⁰ The combination of elastase inhibitor and antimicrobial agents could effectively prevent bacteria colonization and reduce the destructive effects of *P. aeruginosa* exoproteins. Early studies have demonstrated that elastase inhibitors could effectively reduce the extent of corneal melting in an experimental rabbit model of *Pseudomonas* keratitis, yet these inhibitors were not sufficiently active to support their clinical practice.¹¹ However, the correlation between elastase and corneal epithelial barrier in the early stage of infection remains unknown.

The barrier dysfunction played a critical role in the pathogenesis of *P. aeruginosa* keratitis in the early stage. This study was to investigate the role of elastase in the process of corneal epithelial barrier dysfunction caused by the *P. aeruginosa* exoproteins and investigate the molecular details of how corneal epithelial barrier function is modulated. Meanwhile, we aimed at investigating the interaction between corneal epithelial cells and exoproteins. These findings may complement our understanding of the pathophysiology of *P. aeruginosa* corneal infections.

METHODS AND MATERIALS

Preparation and Analysis of *P. aeruginosa* Exoproteins

P. aeruginosa PAO1 strain (ATCC8739) was used as the reference strain for all the experiments. The culture and identification of *P. aeruginosa* PAO1 strain and clinical isolates (kindly donated by the clinical laboratory of the First Affiliated Hospital of Sun-Yat-sen University) were confirmed in the Microbiological Laboratory of Food and Drug Administration of Guangzhou. Standard practices for biosafety level 2 were followed.

The culture supernatant of all *P. aeruginosa* strains was collected at the stationary phase according to the growth curve, then sterilized using 0.22 μm filters and concentrated to 0.5 ml using protein concentrator spin columns (3000 MWCO, GE Healthcare Life Sciences, Chicago, IL, USA). We measured the concentration of exoproteins using the BCA Protein Assay Kit (Thermo Fisher, Waltham, MA, USA). The exoproteins were prepared as a batch and frozen in aliquots (-20°C). The protein profiles of exoproteins were analyzed by shotgun proteomics approach as previously described.¹²

Preparation of Elastase Inhibitor

Synthetic elastase inhibitor was supplied by the pharmaceutical laboratory of Sun-Yat-sen University according to the procedure as described.¹³ The ability of elastase inhibitor to inhibit the proteolytic activity of elastase was tested using Elastin-Congo red (ECR; Sigma-Aldrich, St. Louis, MO, USA) as the substrate. 100 μl elastase inhibitor was added to the

900 μl mixture of 2 $\mu\text{g}/\text{ml}$ exoproteins and ECR buffer (20 mg ECR, 100mM Tris-HCL, pH 7.5), then incubated for 18 hours at 37°C . The liquid supernatant was collected to measure the absorbance value at 495 nm after centrifugation at 16 000 g for 15 minutes. The elastase activity was expressed as the ratio of the OD495 nm and OD600 absorbance value.

Cell Culture

Primary rabbit corneal epithelial cells (CECs) were established by the corneal limbal explant culture method as described.¹⁴ Briefly, the cells were cultured in the Dulbecco's Modified Eagle Medium/Nutrient Mixture F-12 (DMEM-12), supplemented with 5 $\mu\text{g}/\text{ml}$ insulin and 10% fetal calf serum (FCS). The CECs were tested at passage one and identified to be of epithelial lineage via reactivity to K3 and K12 antibodies (Abcam, Cambridge, MA, USA).

Air-Liquid Interface Culture

CECs were maintained at an air-liquid interface (ALI) as previously described.¹⁵ Briefly, 5×10^6 CECs were seeded in 100 μl CECs-ALI growth medium into the apical chamber of the Transwell plate (BD Biosciences, San Jose, California, USA) and 900 μl of CECs-ALI growth medium was added to the basal chamber in all wells containing the inserts. After the cells covered the membrane surface, the CECs-ALI growth medium from the apical chamber was removed and the apical cell surface was exposed to the atmosphere for seven days. The integrity of the cell layer was assessed by measuring baseline transepithelial electrical resistance (TEER).

Cell Viability Assay

Each well of the 24-well plate was inoculated with 8×10^5 cells with a medium change after 24 hours. Before treatment, 0.5 $\mu\text{g}/\text{ml}$, 1 $\mu\text{g}/\text{ml}$, 2 $\mu\text{g}/\text{ml}$, and 4 $\mu\text{g}/\text{ml}$ exoproteins were diluted in PBS to a final volume of 100 μl and was added to 100 μl growth medium. Samples with 8 mM elastase inhibitor were preincubated for five minutes. Cell viability was tested using Cell Counting Kit-8 (CCK8, WST, China). Ten microliters (10 μl) CCK8 was added to each well and incubated for one hour. The optical density was measured at 490 nm on a microplate reader (Biotech, Winooski, USA).

Cell Cytotoxicity Assay

The supernatant of each sample was collected after treatment. The Cytotox-ONE Homogeneous Membrane Integrity Assay (Promega, Australia). was used to measure the amount of lactate dehydrogenase (LDH) in the medium as described.¹⁶

Transepithelial Electrical Resistance (TEER) Analysis

TEER was measured to evaluate the integrity of the corneal epithelial barrier using an EVOM voltmeter (World Precision Instruments, Stevenage, UK).¹⁷ Briefly, after adding 100 μl warmed PBS to the apical chamber to measure baseline resistance, only wells with baseline TEER of greater than 350 Ω/cm^2 were included in the experiments. Exoproteins (2 $\mu\text{g}/\text{ml}$ in CECs-ALI growth medium), elastase inhibitor

(8 mM in CECs-ALI growth medium), and negative control (CECs-ALI growth medium) were added to the apical chamber. TEER was measured at time 0, 1, 2, 3, 4 hours after treatment application. A heating platform was used to maintain CECs-ALI cultures at 37°C during the measurement period. TEER values were measured three times and normalized to the average TEER before the treatment.

Dextran-FITC Permeability Assay

The flux of FITC dextran 4 kDa (Sigma, Saint Louis, USA) was used to represent the paracellular permeability of the corneal epithelial barrier as previously reported.¹⁸ Briefly, after exposure to reagents for two hours, 3 mg/mL of Dextran-FITC was added to the apical chamber and incubated at 37°C for two hours. The supernatant was recovered from the bottom chamber and the amount of Dextran-FITC was determined with a microplate reader (Biotech, Winooski, VT, USA).

Immunofluorescence Staining

After two hours of exposure to exoproteins and elastase inhibitor of CECs-ALI, cells were rinsed with PBS three times and fixed with 25% formalin for 10 minutes. The fixed cells were applied with Triton X-100 (0.1%) and blocked with goat serum for 60 minutes at room temperature. After rinsing in PBS, the cells were incubated with anti-ZO-1 antibodies (Invitrogen, 1:100 dilution) and antioccludin antibodies (Invitrogen, 1:100 dilution) overnight at 4°C. Alexa Fluor 488-conjugated anti-rabbit IgG (1:200) was used as secondary antibodies for one hour and DAPI was applied for 10 minutes. The specimens were examined using a confocal laser scanning microscope (LSM880; Carl Zeiss, Oberkochen, Germany).

Western Blot of Tight Junction Proteins

Cell extracts were prepared in cell lysis buffer as described.¹⁹ Briefly, total protein concentrations were determined by BCA protein assay (Pierce). Equal protein samples were electrophoresed on 12% SDS-PAGE gels. After being blocked with 5% milk, the membranes were incubated with anti-ZO-1 antibodies (Invitrogen, 1:500 dilution) and antioccludin antibodies (Invitrogen, 1:500 dilution) overnight at 4°C. Goat anti-rabbit IgG horseradish peroxidase (HRP, Abcam) were used as secondary antibodies. Luminescence was detected using the ECL western blotting system (Fujifilm, Tokyo, Japan).

Enzyme-Linked Immunosorbent Assay (ELISA)

The conditional media was centrifuged at 16 000 g for 15 minutes and the supernatants were collected as described previously.²⁰ The level of proinflammation factors was examined according to the instructions of the ELISA kit: IL-6, IL-1 β , IL-8, and TNF- α (R&D Systems, Minneapolis, MN, USA). Results are presented as mean level of cytokines in pg/ml per mg cell lysate \pm SE ($n = 3$).

Animals and Experiment Groups

C57BL/6J mice (male, four weeks old) were bought from the Experimental Animal Research Center of Sun-Yat-sen University. All animals' use and care strictly conformed to

the ARVO statements for the Use of Animals in Ophthalmic and Vision Research, and this study was formally reviewed and approved by the first affiliated hospital of Sun-Yat-sen University Animal Care and Ethics Committee (2021–051).

Mice were divided into four groups randomly and treated separately by 40 μ g/ml exoproteins, 16 mM elastase inhibitor (10 μ l/eye) or 10 μ l PBS as controls three times each day for two days. The ocular surface clinical signs were observed through the slit lamp microscope. Animals were examined clinically for signs of corneal epithelial defects 10 minutes after last exoproteins topical challenge each day. Tissue specimens including corneal tissues were fixed in acetone for whole mount staining. Five mice per group were used in each experiment. Some of the mice were killed following these assessments, and the corneas of these mice were collected and stored at -80°C for further analysis.

Fluorescein Sodium Staining

Two microliters (2 μ l) of 0.1% sodium fluorescein solution were dropped into the conjunctival sac of mouse (without anesthesia). After three blinks, excess fluorescein was wiped from the lateral tear meniscus. Then, corneal epithelial damage was observed and imaged with a cobalt blue filter under a slit lamp microscope (YZ5S, Six-six visual Inc., Suzhou, Jiangsu, China). Images were acquired by two independent technicians and quantification of corneal defects were carried out by ImageJ software (USA). The covering area of corneal defects (%) = (fluorescein sodium positive area/the whole cornea) \times 100%.

Hematoxylin and Eosin Staining

After the animals were killed, the eyes were dissected and fixed in 4% paraformaldehyde overnight and embedded in paraffin. The tissue sections (5 μ m) were deparaffinized and stained with hematoxylin for one minute and eosin for two minutes. After that, the sections were mounted using mounting medium and examined under a light microscope (Olympus BH2, Tokyo, Japan).

Immunostaining

Cryostat sections (6 μ m) of mice eyes were fixed in 4% paraformaldehyde for 20 minutes. The samples were washed three times with PBS, followed by incubation in 0.2% Triton X-100 for 10 minutes. After rinsing three times with PBS for five minutes each and preincubation with 2% bovine serum albumin (BSA) for one hour at room temperature, sections were incubated with anti-ZO-1 (1:100, Invitrogen), occludin (1:100, Invitrogen) primary antibodies at 4°C overnight. After three washes with PBS for 10 minutes each, they were incubated with Alexa Fluor 488-conjugated secondary antibody (donkey anti-rabbit, goat, rat, or mouse IgG, 1:300, Life Technologies, Carlsbad, CA, USA) for one hour at room temperature. After three additional PBS washes for five minutes, the samples were counterstained with DAPI and then mounted for analysis under the confocal laser scanning microscope (LSM 780, Zeiss).

Scanning Electron Microscopy

One corneal epithelial sample was obtained from each eye. Fixed materials were dehydrated through a series of ethanol. Whole corneas were placed in amyl acetate after being

TABLE. Identification of Supernant Proteins from *P. aeruginosa* PAO1 and Clinical Isolate Strain

Protein ID	Protein Identification	Gene Name	MW (kDa)	Unique Peptides	PAO1		CI		
					IBAQ	seq.cov (%)	Unique Peptides	IBAQ	seq.cov (%)
P14756	Elastase	lasB	53.7	7	45941000	24.2	10	335240000	33.5
V6AIL0	Flagellin	fliC	49.2	3	7314400	22.4	1	7319800	35.8
A0A6G7LC28	lasA protease	lasA	44.6	5	37567000	22.2	6	60375000	31.5
A0A1G9YY14	Serine protease SohB	SohB	57.5	1	103640000	21.2	4	105060000	38.7
A0A1H0BUC5	Type VI secretion system protein VasJ	VasJ	51	1	3166600	25.7	1	1906600	20.3
A0A0A8RLM1	Pilin	pilA	61.2	1	5742600	28.8	1	104230000	29.1
PA1249	Alkaline protease	AprA	50.4	3	50805000	16.4	2	86477000	28.1
A0A6H1QHQ9	PASP protease	PASP	20.8	5	22289000	18.4	3	43224700	23.3
W6QV37	Lon protease	lon1	33	3	3499200	15.2	5	4236500	18.4

Proteomic profiling of exoproteins from *Pseudomonas aeruginosa* PAO1 and clinical isolated strain (CI). Proteins were identified by trypsin digest and shotgun proteomics approach. Protein gene name and molecular weight were from the *Pseudomonas* Genome Database. (For detailed data, see supplementary material.)

treated in a critical point drying apparatus (Hitachi HCP2, Hitachi, Japan) and then sputter coated with gold with an auto fine coater (JEOL JFC-1600, JEOL, Japan) and examined using a scanning electron microscope (Stereoscan 250 Mk3, Cambridge, UK).

Statistical Analysis

Data are expressed as mean \pm standard error of mean (SEM). The TEER, permeability assay, cell cytotoxicity assay experiments were performed using three biological replicates. Differences between groups were assessed by *t*-test. Statistical analysis of inhibition of elastase inhibitor was performed using one-way ANOVA and significance was determined by Tukey honest significance difference test ($P < 0.05$).

RESULTS

Comparative Analysis of Exoproteins From *P. aeruginosa* PAO1 and Clinical Isolated Strain (CI)

To determine the composition of *P. aeruginosa* exoproteins and whether differences between *P. aeruginosa* PAO1 strain and clinical isolated (CI) strain exist, we investigated extracellular protein profiles of exoproteins using a shotgun proteomics approach. 294 proteins were identified including elastase B (lasB), alkaline protease, the serine protease, and some predicted secreted proteins (Table). 194 (66%) proteins were identified in both PAO1 and clinical isolated strain, while 29 (10%) proteins and 71 (24%) proteins were identified in PAO1 and clinical isolated strain alone, respectively. Compared with laboratory-adapted strain PAO1 (24.2%), the sequence coverage of elastase of *P. aeruginosa* clinical isolate strain (33.5%) was higher, which goes in line with previous studies that much higher levels of elastase have been detected in the sputum of cystic fibrosis patients.²⁰ The infection microenvironment can influence the expression of virulence factors in *P. aeruginosa*. As shown in Supplementary Figure S4, the elastase activity of the *P. aeruginosa* clinical isolated strain is higher than the laboratory adapted standard strain PAO1 (ATCC 8739). The high level of elastase may explain why the clinical isolates are more virulent than the laboratory adapted strain PAO1. These results supported that elastase specifically contribute to the virulence of *P. aeruginosa*, which play a critical role in the pathogenesis of *P. aeruginosa* infection.

The Effects of *P. aeruginosa* Exoproteins on Bioactivities of CECs Under Different Concentrations and Times

In the growth curve assay, the inhibition effect of 0.5 μ g/ml, 1 μ g/ml, 2 μ g/ml, and 4 μ g/ml on cell proliferation was observed. The *P. aeruginosa* exoproteins showed suppression on proliferation of CECs compared to the control at 0.5 μ g/ml and caused a strong and concentration-dependent decrease in proliferation of CECs ($P < 0.05$). The proliferation of CECs remains slow at 2 μ g/ml. Significant inhibition of proliferation of CECs occurred at 4 μ g/ml (Fig. 1A). After the CECs were treated with 2 μ g/ml exoproteins for 24 hours, exoproteins exert a time-dependent damage effect on the viability of CECs. Compared with the control group, in the presence of 2 μ g/ml exoproteins, the relative viability of the CECs began to decrease significantly at two hours and reduces to approximately 50% at eight hours, while an almost loss of viability occurred at 24 hours (Fig. 1B). As shown in Supplementary Figure S3, the cell detachment process began with small gaps in the monolayers, which enlarged until all cells were detached completely and formed suspended aggregates (black arrows). The CECs at the edges appear to curl up and the cell-free areas enlarged in a time-dependent manner in treated cells after the application of 2 μ g/ml exoproteins for two hours. We observed half of the CECs showed cell detachment within eight hours (Fig. 1C).

Exoproteins Disrupted the Barrier Structure and Function of CECs-ALI Cultures and the Destructive Effect Was Relieved by Elastase Inhibitor

We measured the transepithelial electrical resistance (TEER) and the flux of Dextran-FITC tracers across CECs-ALI cultures to assess the corneal epithelial barrier function. Our study showed that 2 μ g/ml exoproteins disrupted the barrier function in a time-dependent manner evidenced by increased permeability of FITC-dextran ($P < 0.05$). After 2 μ g/ml exoproteins applied to CECs-ALI cultures for two hours, there was a 2.18 fold increased permeability of FITC-dextran, and TEER value decreased from 323.2 ± 2.7 to $124 \pm 6.8 \Omega \text{ cm}^2$ compared with that of the control group, indicating that exoproteins had a destructive effect on the barrier function of the CECs-ALI cultures (Fig. 2A). Additionally, the TEER value was increased to $227 \pm 3.4 \Omega \text{ cm}^2$ by 8 mM elastase inhibitor treatment compared with the exoproteins

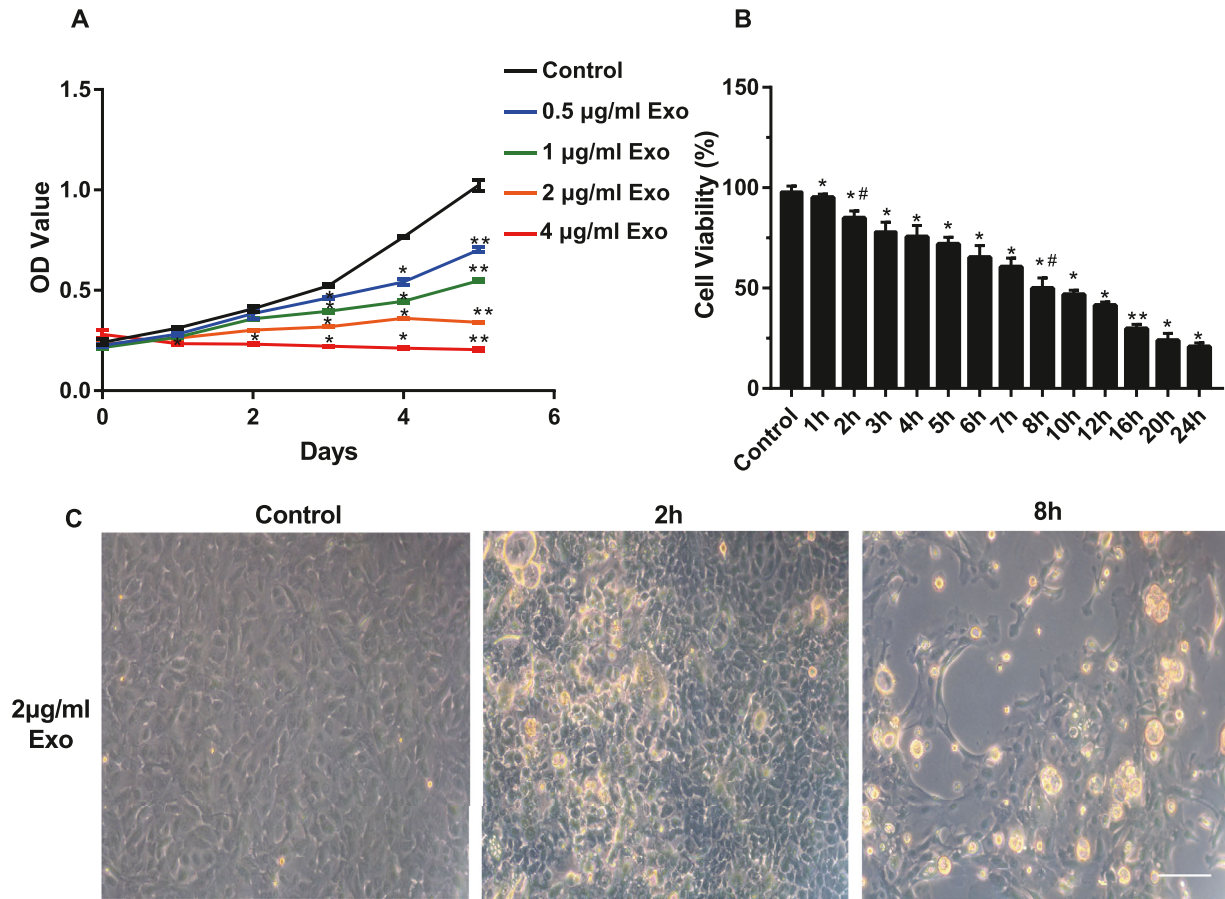


FIGURE 1. The damage effects of *Pseudomonas aeruginosa* exoproteins on rabbit corneal epithelial cells. **(A)** CCK8 was used to analyze the effect of exoproteins on rabbit corneal epithelial cell proliferation at different concentrations. **(B)** Changes in the viability of rabbit corneal epithelial cells after treatment with 2 µg/ml exoproteins at different times using WST assay. **(C)** Morphological changes of rabbit corneal epithelial cells were observed by light microscope after treatment with 2 µg/ml of exoproteins for two hours and eight hours. Scale bar = 10 0µm. The values are shown as mean ± SD, analyzed by one-way ANONA. **P* < 0.05 versus control group, ***P* < 0.01 versus control group, #*P* < 0.01 versus one hour group (*n* = 3).

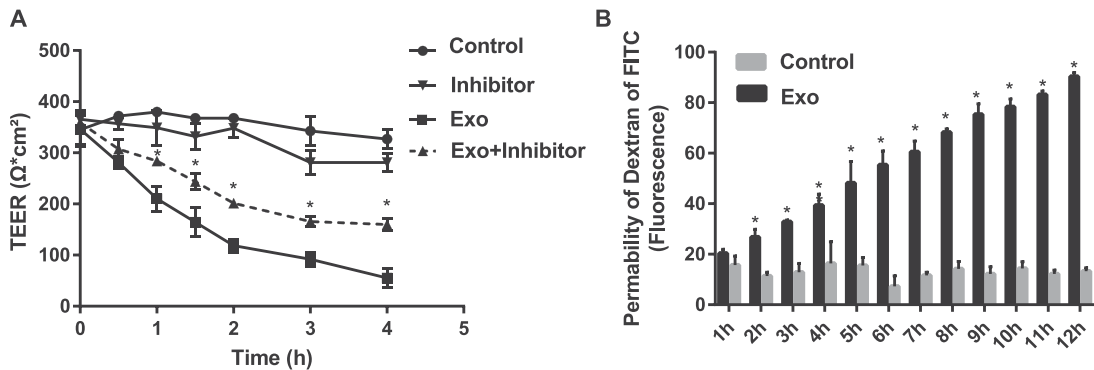


FIGURE 2. Effect of elastase inhibitor on the barrier function of corneal epithelial cell air-liquid interface cultures exposed to exoproteins. **(A)** After application of exoproteins for different times, infiltration of Dextran-FITC fluorescence intensity at the basal chamber was detected to evaluate paracellular permeability of CECs air-liquid interface cultures; **(B)** After application of exoproteins and elastase inhibitor, the transepithelial electrical resistance (TEER) was detected to evaluate the barrier function of the CECs air-liquid interface cultures. (1) Control group: PBS; (2) Exo group: 2 µg/ml exoproteins; (3) Inhibitor group: 8 mM Inhibitor; (4) Exo + Inhibitor group: 2 µg/ml exoproteins + 8 mM inhibitor. The values are shown as mean ± SD for *n* = 3. **P* < 0.05 versus control group, ***P* < 0.01 versus control group, ANONA, followed by Tukey HSD post hoc test.

group, suggesting that the elastase inhibitor could relieve the destructive impact of exoproteins on the barrier function of

CECs-ALI cultures, However, the TEER did not restore to the normal level compared with the control group (Fig. 2B).

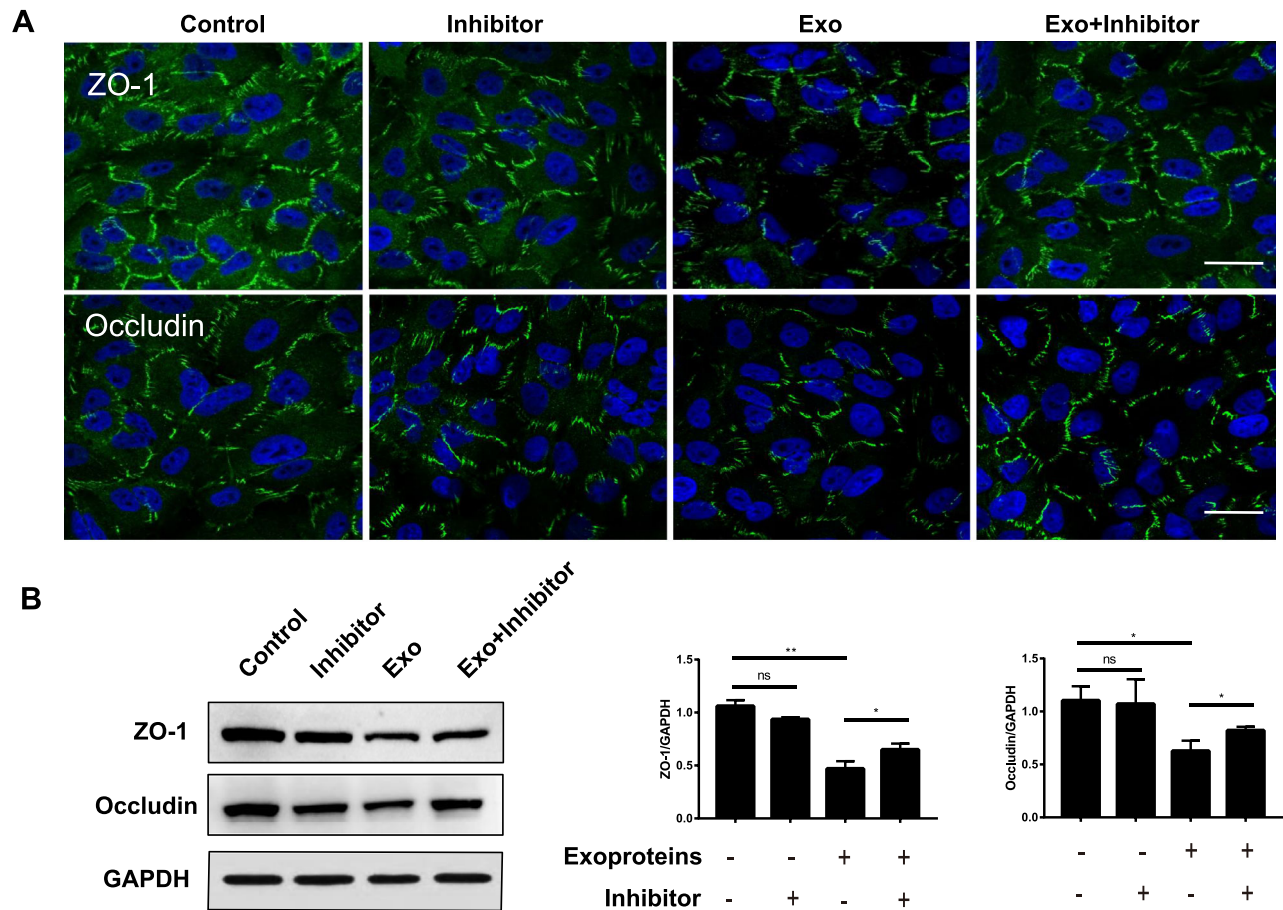


FIGURE 3. Effect of elastase inhibitor on the tight junction of corneal epithelial cells after treatment with exoproteins. (A) Immunofluorescent staining of rabbit corneal epithelial cells ZO-1 (green), occludin (green), and nuclei (blue) after different treatments of both exoproteins and inhibitor for two hours. (B) Western blot analysis and quantitative analysis of ZO-1 and occludin expression in rabbit corneal epithelial cells two hours after different treatments. Scale bar = 20 μ m. The values are shown as mean \pm SD, analyzed by one-way ANOVA. ns $P > 0.05$ versus control group, * $P < 0.05$, ** $P < 0.01$ ($n = 3$).

Inhibition of Elastase Could Relieve the Disruption and Degradation of Tight Junction Proteins Caused by *P. aeruginosa* Exoproteins

We examined the expression and location of tight junction protein after treatment of 2 μ g/ml exoproteins. The location of tight junction protein ZO-1 and occludin were examined by immunostaining assay. Our results showed that exoproteins produced a discontinuous and less intense localization of ZO-1 and occludin at the cell periphery compared to the control (Fig. 3). Compared with the control group, application of exoproteins caused significant degradation of tight junction protein ZO-1 ($P = 0.0124$) and reduction in occludin protein levels ($P = 0.0253$); the expression levels of ZO-1 and occludin were increased after treatment with elastase inhibitor compared with the exoproteins group ($P < 0.05$).

Damage Effects of Exoproteins on CECs Involves the Induction of Cell Detachment and Apoptosis

We examined the apoptosis rate and morphological change of CECs two hours after treatment with exoproteins to assess the effects of exoproteins on the corneal epithelial mono-

layers with or without elastase inhibitor. The rabbit corneal epithelial cells showed polygonal morphology in normal condition. After the application of exoproteins for two hours, the CECs at the edge began to curl up and formed the suspended aggregates, similar to the phenomenon known as anoikis (Fig. 4A). To determine whether apoptosis was involved in the process, we used flow cytometry to assess the apoptosis rate of CECs. Compared with the control group, the percentage of cell apoptosis increased from $3.16 \pm 1.3\%$ to $30.2 \pm 3.8\%$ after treated with exoproteins, indicating that cell apoptosis plays a critical role in the early stage of corneal injury caused by exoproteins. Meanwhile, the apoptosis rate decreased to $7.26 \pm 1.3\%$ after treatment with the elastase inhibitor (Fig. 4B).

Inhibition of the Elastase Decreased the Release of Proinflammatory Cytokines of CECs After Application of Exoproteins

To investigate the effect of *P. aeruginosa* exoproteins on the expression of proinflammatory factors with or without elastase inhibitor, we measured the expression of IL-1, IL-6, IL-8, and TNF- α by enzyme-linked immunosorbent assay. Our results showed that exoproteins induced a clear and strong

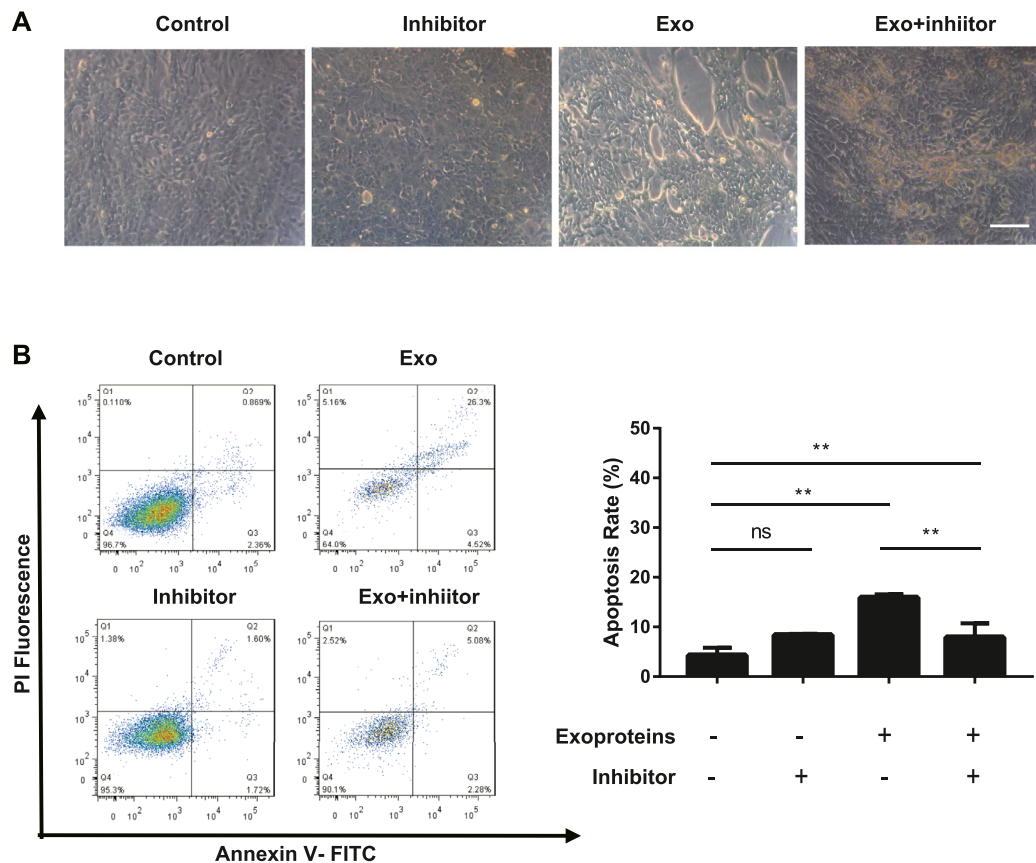


FIGURE 4. Effect of elastase inhibitor on corneal epithelial cell morphology and apoptosis rate after treatment with exoproteins. **(A)** Morphological changes of rabbit corneal epithelial cells under the light microscope after two hours treatment. **(B)** Flow cytometry was used to detect the apoptosis rate of corneal epithelial cells after different treatments with exoproteins and elastase inhibitor for two hours. **(1)** Control group: PBS. **(2)** Exo group: 2 μ g/ml exoproteins. **(3)** Inhibitor group: 8 mM inhibitor. **(4)** Exo + Inhibitor group: 2 μ g/ml exoproteins + 8 mM inhibitor. Scale bar = 100 μ m. The values are shown as mean \pm SD, analyzed by one-way ANOVA. ns $P > 0.05$ versus control group, ** $P < 0.01$ ($n = 3$).

inflammatory response. Compared with the control group (201.35 ± 21.06 pg/ml), the level of IL-1 β increased significantly to 724.29 ± 23.15 pg/ml after application of exoproteins for two hours, while it significantly decreased to 423.29 ± 17.34 pg/ml with elastase inhibitor (Fig. 5). Besides, IL-6, TNF- α , and IL-8 levels decreased after application of the elastase inhibitor compared with the exoproteins group ($P < 0.05$).

Inhibition of the Elastase Ameliorated Corneal Epithelial Defects Induced by Exoproteins in Murine Model In Vivo

To investigate the virulence contribution of elastase in exoproteins-induced corneal damage in vivo, we examined the effects of exoproteins in the presence or absence of elastase inhibitor on the corneal epithelium in a murine model. Slit lamp examination, histopathological analysis, and the staining of tight junction proteins ZO-1 were performed in these animal studies. As shown in Supplementary Figure S1, compared with PBS treated controls, the topical administration of exoproteins for 24 hours resulted in mild corneal epithelial defects. There were many widespread punctuate and confluent staining on the corneas treated with exoproteins for 48 hours. The result of H&E staining showed jagged

epithelial surface and thinner corneal epithelial layer in the corneas with exoproteins exposure compared with the control group.

As shown in Figure 6, compared with the control group, scabrous corneal surface and diffused punctuate staining were observed on the mouse corneas treated with exoproteins compared with the control group. The fluorescein sodium staining used to measure the corneal surface disrupted areas showed that the average corneal epithelial defected area in the mouse cornea exposed to exoproteins was $23.5 \pm 5.8\%$, significantly higher than the PBS control group ($1.2 \pm 0.16\%$). The defected area decreases to $13.2 \pm 2.4\%$ ($P < 0.05$) after application of elastase inhibitor. H&E staining of exoproteins-treated corneas revealed disorganized apical epithelial layers and thinner corneal epithelial multiple layers compared with the smooth epithelial surface in the control group ($P < 0.05$). The application of elastase inhibitor partly restores structural integrity of the corneas. To further evaluate the integrity of ocular surface epithelial barrier, immunofluorescence staining was performed to evaluate the integrity of major tight junction proteins. Compared with the control group, the IF staining of tight junction proteins ZO-1 and occludin displayed discontinuous staining at the epithelial cell borders in exoproteins-treated corneas, suggesting compromised corneal epithelial barrier, while the abundance and integrity of these

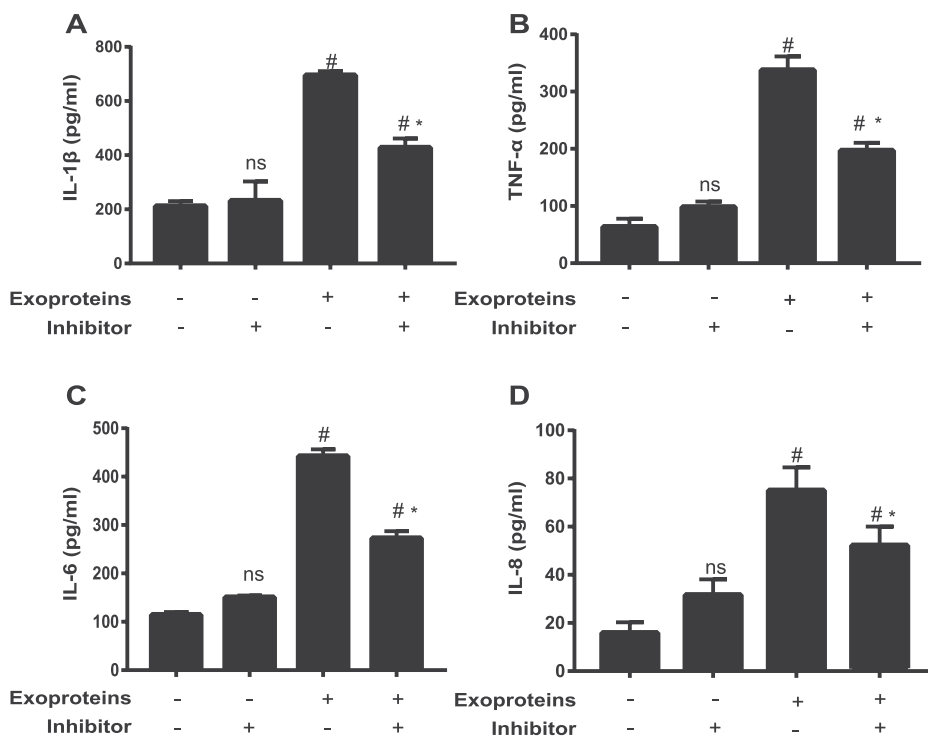


FIGURE 5. The effect of *P. aeruginosa* exoproteins on the expression of proinflammatory factors with or without elastase inhibitor. The expression of IL-1 β (A), TNF- α (B), IL-6 (C), and IL-8 (D) were measured by enzyme-linked immunosorbent assay. The values are shown as mean \pm SD, analyzed by one-way ANOVA. # P < 0.01 versus control group, ns P > 0.01 versus control group, * P < 0.05 versus Exo group (n = 3).

tight junction proteins was increased after application of elastase inhibitor (Supplementary Fig. S2). Scanning electron microscopy (SEM) has been used to evaluate ultrastructural changes of corneal epithelial cells. Compared with the corneas with a high density of microvilli in the control group, scarce and incomplete microvilli were observed in the corneas treated with exoproteins, while some surface cells retract from their cell contacts leaving retraction fibrils. As shown in Fig. 7, white arrows indicate some cell edges are peeling up. The results further confirmed that elastase plays a critical role in the disruptive effects of exoproteins on the corneal epithelial barrier.

DISCUSSION

P. aeruginosa keratitis is one of the most aggressive and destructive diseases of the cornea. The infection is hard to control because the corneal ulcer develops rapidly, and corneal perforation may occur in 24 hours even when treated with strong antibiotics.²¹ New therapies to control the corneal damage are urgently needed. Intact corneal structure and barrier function are critical to maintain corneal epithelial homeostasis and defense against microbial attack.²² Targeting corneal epithelial barrier protection and antiviral approaches are promising strategies to control the progress of *P. aeruginosa* infection.²³ However, much less is known about the factors that compromise that resistance and render the cornea susceptible to infection. Previous studies on the mechanism of corneal ulceration indicated that severe corneal ulceration and extensive dissolution of the stroma were associated with the production of *P. aeruginosa* exoproteins during infection.^{24,25} In this

study, we established the multilayered CECs barrier model in vitro successfully to assess the effect of exoproteins on the corneal epithelial barrier. Our findings showed *P. aeruginosa* exoproteins induced a severe degradation of tight junction proteins and disrupted corneal epithelial barrier structure.

The concerted action of exoproteins plays a critical role in the pathogenicity of *P. aeruginosa*.²⁶ Exoproteins that are associated with invasion are commonly proteases. Microbiome studies showed that *P. aeruginosa* elastase is a major elastolytic enzyme and has highly proteolytic activity. Other proteases such as alkaline protease, the serine protease, and *P. aeruginosa* aminopeptidase (PAAP) are thought to have little proteolytic activity.^{27,28} Previous study showed that *P. aeruginosa* elastase was elevated in AES (Australian epidemic strain) culture compared with laboratory-adapted strain PAO1.²⁹ In our study, the secretome analysis of *P. aeruginosa* showed Two hundred ninety-four proteins could be identified, including elastase B (lasB), the serine protease, and some predicted secreted proteins. One hundred ninety-four proteins were identified in both PAO1 and clinical isolated strain. Compared with laboratory-adapted strain PAO1, *P. aeruginosa* clinical isolated strain showed an elevated level of elastase consistent with previous research.²⁹ It indicates that elastase plays a critical role in the pathogenesis of *P. aeruginosa* infection and is a potential target to be explored. However, the exact role and contribution of elastase in this process remain unknown and the mechanism of elastase on the epithelial barrier has not been fully elucidated. In our study, we have prepared synthetic inhibitors for the elastase based on the previous research. To investigate the role of elastase in the process of corneal

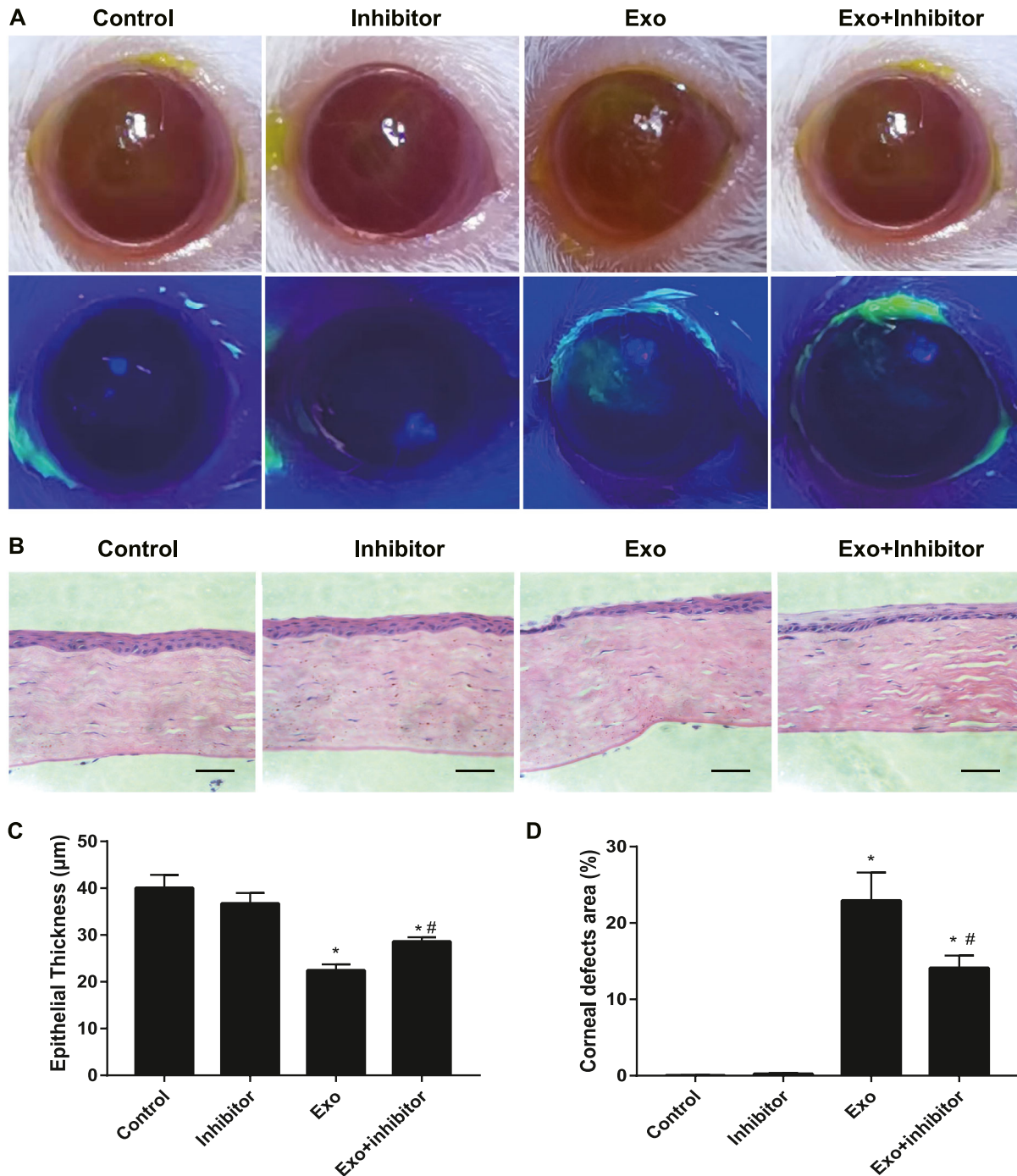


FIGURE 6. The inhibition of elastase improved the corneal epithelial defects induced by exoproteins. (A) Representative images of fluorescein sodium staining showing corneal epithelial defects in mice treated with 40 µg/ml exoproteins and/or 16 mM elastase inhibitor for 48 hours ($n = 3$ mice/group). (B) The images of HE staining of cornea epithelium treated after different treatment. (C) The quantitative analysis of corneal epithelial defect area and (D) epithelial thickness after different treatment using ImageJ software. Scale bar = 100 µm; * $P < 0.05$ versus Control group, # $P < 0.05$ versus Exo group ($n = 3$).

damage, we examined the effects of the elastase inhibitor on the barrier structure and function after the application of *P. aeruginosa* exoproteins. Our findings indicated that 8 mM elastase inhibitor could protect the CECs-ALI culture barrier function compromised by 2 µg/ml exoproteins. Although the CECs-ALI culture barrier function could not restore to the normal level compared to the untreated controls because

of the multifactorial virulence of *P. aeruginosa* exoproteins, the elastase inhibitor offers a new therapeutic strategy in the early stage of *P. aeruginosa* infections.

Next, we examined the effects of elastase inhibitor on exoproteins-induced damage on the corneal epithelium in a murine model. In agreement with our previous studies *in vitro*, compared with the control group, the addition of

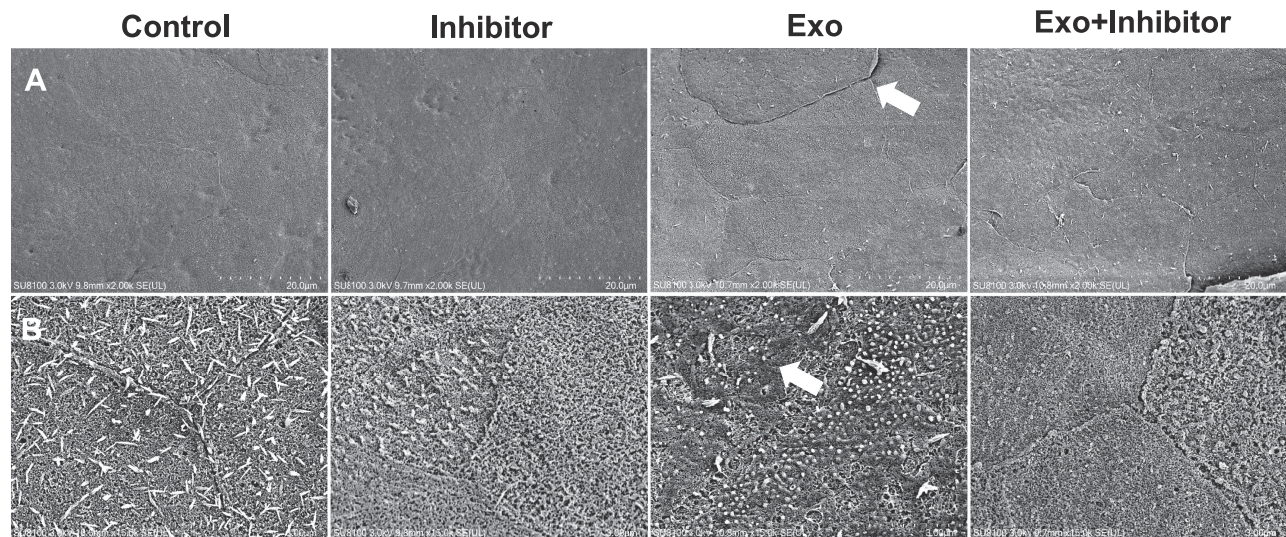


FIGURE 7. Scanning electron microscopy of the corneas exposed to exoproteins with or without elastase inhibitor for 48 hours. **(A)** Normal superficial cells of corneal epithelium. After application of exoproteins for 48 hours, some surface cells retract from their cell contacts, leaving retraction fibrils. White arrows indicate some cell edges are peeling up. Scale bar = 20 μm . **(B)** A high density of microvilli and microplicae is observed in the control group. In the exoproteins-treated group, microvilli are scarce and degenerated. Surface cells have lost their microvilli and show membrane wrinkling (white arrow). Scale bar = 3 μm .

40 $\mu\text{g}/\text{ml}$ exoproteins induced mild epithelial defects and thinner epithelial layer, while inhibition of elastase partly restored structural integrity and increased the abundance of tight junction proteins of the corneas. The observed effects may be ascribed to the degradation of collagen, elastin, and tight junction proteins by elastase resulting in tissue disintegration and the loss of cytoskeletal structures. The results further confirmed that elastase plays a critical role in the disruptive effects of exoproteins on the corneal epithelial barrier.

Previous studies have shown that cultured corneal epithelial cells are vulnerable to *P. aeruginosa* infection.³⁰ The interaction between corneal epithelial cells and exoproteins remains unclear. In our study, we examined the effects of *P. aeruginosa* exoproteins on corneal epithelial cells and elucidate the exact role and contribution of elastase in the process by using a synthetic elastase inhibitor. Loss of cell viability and changes in the cytoskeletal morphology were observed in response to exoproteins in a time-dependent manner. We noticed the total loss of cells following a 24 hour incubation with 2 $\mu\text{g}/\text{ml}$ exoproteins. Eight millimolar (8mM) elastase inhibitor could prevent the total loss of cell viability triggered by exoproteins and increased the relative survival rate of corneal epithelial cells. The elastase inhibitor showed no toxicity toward corneal epithelial cells. However, the full recovery of corneal epithelial cell viability could not be observed because of the multifactorial virulence of *P. aeruginosa* exoproteins. Only 68.32% of the cells remained viable in the presence of sufficient elastase inhibitors. Meanwhile, we noticed that exoproteins induced a clear and strong inflammatory response, while inhibition of elastase partly reduced the expression of proinflammatory cytokines. Different mechanisms of cell death may occur during *P. aeruginosa* infection. Pyroptosis is a type of proinflammatory programmed cell death, which may be involved in the early process of corneal resistance to infection and removal of *P. aeruginosa* as previously reported.³¹ Exoproteins (including superantigens and

cytolysins) induced proinflammatory signals from epithelial cells have been well characterized in *Staphylococcus aureus* infection.³² The pathogenesis of *P. aeruginosa* at the corneal epithelial surface remains unclear. Exoproteins may enhance the transport of superantigens across the epithelial barrier by either direct toxicity or inflammatory activation of epithelial cells.³² Future studies are planned to elucidate the mechanism of exoproteins on the corneal epithelial surface. There are some limitations in this study; purified elastase is required to elucidate the exact role of elastase in the process of *P. aeruginosa* corneal infection. While our result confirmed that elastase contributed to the corneal epithelial barrier disruption, the details of mechanistic effects remained to be explored. Future studies are planned to elucidate the mechanism behind elastase in the pathogenesis of *P. aeruginosa* infection using lasB mutants.

In conclusion, our study showed *P. aeruginosa* exoproteins directly contribute to the disruption of the corneal epithelial barrier in a manner correlated with the elastase activity. Inhibition of elastase could protect the corneal epithelial barrier function by reducing degradation and reorganization of tight junction proteins, decreasing the expression of proinflammatory cytokines, and improving viability of CECs. Antielastase treatment and targeted corneal epithelial barrier protection could be avenues of novel therapies in the treatment of *P. aeruginosa* corneal infection.

Acknowledgments

The authors thank the Microbiological Laboratory of Food and Drug Administration of Guangzhou and the clinical laboratory of the First Affiliated Hospital of Sun-Yat-sen University for their support.

Disclosure: **Y. Li**, None; **Y.W. Wang**, None; **C.W. Li**, None; **D.P. Zhao**, None; **Q.Y. Hu**, None; **M. Zhou**, None; **M. Du**, None; **J. Li**, None; **P.X. Wan**, None

References

- Ruffin M, Brochiero E. Repair process impairment by *P. aeruginosa* in epithelial tissues: Major features and potential therapeutic avenues. *Front Cell Infect Microbiol.* 2019;9:182.
- Evans DJ, Fleiszig SM. Why does the healthy cornea resist *P. aeruginosa* infection? *Am J Ophthalmol.* 2013;155(6):961–970.e2.
- Stern GA, Lubniewski A, Allen C. The interaction between *P. aeruginosa* and the corneal epithelium. An electron microscopic study. *Arch Ophthalmol.* 1985;103(8):1221–1225.
- Klotz SA, Au YK, Misra RP. A partial-thickness epithelial defect increases the adherence of *P. aeruginosa* to the cornea. *Invest Ophthalmol Vis Sci.* 1989;30(6):1069–1074.
- Alarcon I, Tam C, Mun JJ, LeDue J, Evans DJ, Fleiszig SM. Factors impacting corneal epithelial barrier function against *P. aeruginosa* traversal. *Invest Ophthalmol Vis Sci.* 2011;52(3):1368–1377.
- Jurado-Martín I, Sainz-Mejías M, McClean S. *P. aeruginosa*: An audacious pathogen with an adaptable arsenal of virulence factors. *Int J Mol Sci.* 2021;22(6):3128.
- Strateva T, Mitov I. Contribution of an arsenal of virulence factors to the pathogenesis of *P. aeruginosa* infections[J]. *Ann Microbiol.* 2011;61(4):717–732.
- Azghani AO, Miller EJ, Peterson BT. Virulence factors from *P. aeruginosa* increase lung epithelial permeability[J]. *Lung.* 2000;178(5):261–269.
- Clark CA, Thomas LK, Azghani AO. Inhibition of protein kinase C attenuates pseudomonas aeruginosa elastase-induced epithelial barrier disruption. *Am J Respir Cell Mol Biol.* 2011;45(6):1263–1271.
- Galdino ACM, de Oliveira MP, Ramalho TC, de Castro AA, Branquinha MH, Santos ALS. Anti-virulence strategy against the multidrug-resistant bacterial pathogen *P. aeruginosa*: Pseudolysin (elastase B) as a potential druggable target. *Curr Protein Pept Sci.* 2019;20(5):471–487.
- Burns FR, Paterson CA, Gray RD, Wells JT. Inhibition of *P. aeruginosa* elastase and Pseudomonas keratitis using a thiol-based peptide. *Antimicrob Agents Chemother.* 1990;34(11):2065–2069.
- Scott NE, Hare NJ, White MY, Manos J, Cordwell SJ. Secretome of transmissible *P. aeruginosa* AES-1R grown in a cystic fibrosis lung-like environment. *J Proteome Res.* 2013;12(12):5357–5369.
- Szamosvári D, Reichle VF, Jureschi M, Böttcher T. Synthetic quinolone signal analogues inhibiting the virulence factor elastase of *P. aeruginosa*. *Chem Commun (Camb).* 2016;52(92):13440–13443.
- Yan H, Wang Y, Shen S, Wu Z, Wan P. Corticosteroids effects on LPS-induced rat inflammatory keratocyte cell model. *PLoS One.* 2017;12(4):e0176639.
- Leduc D, Beaufort N, de Bentzmann S, Rousselle JC, Namane A, Chignard M, Pidard D. The *P. aeruginosa* LasB metalloproteinase regulates the human urokinase-type plasminogen activator receptor through domain-specific endoproteolysis. *Infect Immun.* 2007;75(8):3848–3858.
- Yu H, He X, Xie W, Xiong J, Sheng H, Guo S, Huang C, Zhang D, Zhang K. Elastase LasB of *P. aeruginosa* promotes biofilm formation partly through rhamnolipid-mediated regulation. *Can J Microbiol.* 2014;60(4):227–235.
- Li J, Ramezanzpour M, Fong SA, Cooksley C, Murphy J, Suzuki M, Psaltis AJ, Wormald PJ, Vreugde S. *P. aeruginosa* exoprotein-induced barrier disruption correlates with elastase activity and marks chronic rhinosinusitis severity. *Front Cell Infect Microbiol.* 2019;9:38.
- Jiao J, Yang J, Li J, Li Y, Zhang L. Hypertonic saline and seawater solutions damage sinonasal epithelial cell air-liquid interface cultures. *Int Forum Allergy Rhinol.* 2020;10(1):59–68.
- Marino GK, Santhiago MR, Santhanam A, Lassance L, Thangavadiel S, Medeiros CS, Bose K, Tam KP, Wilson SE. Epithelial basement membrane injury and regeneration modulates corneal fibrosis after pseudomonas corneal ulcers in rabbits. *Exp Eye Res.* 2017;161:101–105.
- De Paiva CS, Chotikavanich S, Pangelinan SB, 3rd Pitcher JD, Fang B, Zheng X, Ma P, Farley WJ, Siemasko KF, Niederkorn JY, Stern ME, Li DQ, Pflugfelder SC. IL-17 disrupts corneal barrier following desiccating stress. *Mucosal Immunol.* 2009;2(3):243–253.
- Suleman L. Extracellular bacterial proteases in chronic wounds: A potential therapeutic target? *Adv Wound Care (New Rochelle).* 2016;5(10):455–463.
- Hilliam Y, Kaye S, Winstanley C. *P. aeruginosa* and microbial keratitis. *J Med Microbiol.* 2020;69(1):3–13.
- Kantyka T, Plaza K, Koziel J, Florczyk D, Stennicke HR, Thogersen IB, Enghild JJ, Silverman GA, Pak SC, Potempa J. Inhibition of Staphylococcus aureus cysteine proteases by human serpin potentially limits staphylococcal virulence. *Biol Chem.* 2011;392(5):483–489.
- Oka N, Suzuki T, Ishikawa E, Yamaguchi S, Hayashi N, Gotoh N, Ohashi Y. Relationship of virulence factors and clinical features in keratitis caused by *P. aeruginosa*. *Invest Ophthalmol Vis Sci.* 2015;56(11):6892–6898.
- Sauvage S, Hardouin J. Exoproteomics for better understanding *P. aeruginosa* virulence. *Toxins (Basel).* 2020;12(9):571.
- El Zowalaty ME, Al Thani AA, Webster TJ, El Zowalaty AE, Schweizer HP, Nasrallah GK, Marei HE, Ashour HM. *P. aeruginosa*: Arsenal of resistance mechanisms, decades of changing resistance profiles, and future antimicrobial therapies. *Future Microbiol.* 2015;10(10):1683–1706.
- Oldak E, Trafny EA. Secretion of proteases by *P. aeruginosa* biofilms exposed to ciprofloxacin. *Antimicrob Agents Chemother.* 2005;49(8):3281–3288.
- Mochizuki Y, Suzuki T, Oka N, Zhang Y, Hayashi Y, Hayashi N, Gotoh N, Ohashi Y. *P. aeruginosa* MucD protease mediates keratitis by inhibiting neutrophil recruitment and promoting bacterial survival. *Invest Ophthalmol Vis Sci.* 2014;55(1):240–246.
- Scott NE, Hare NJ, White MY, Manos J, Cordwell SJ. Secretome of transmissible *P. aeruginosa* AES-1R grown in a cystic fibrosis lung-like environment. *J Proteome Res.* 2013;12(12):5357–5369.
- Saraswathi P, Beuerman RW. Corneal biofilms: From planktonic to microcolony formation in an experimental keratitis infection with *P. aeruginosa*. *Ocul Surf.* 2015;13(4):331–345.
- Qu W, Wang Y, Wu Y, Liu Y, Chen K, Liu X, Zou Z, Huang X, Wu M. Triggering receptors expressed on myeloid cells 2 promotes corneal resistance against *P. aeruginosa* by inhibiting caspase-1-dependent pyroptosis. *Front Immunol.* 2018;9:1121.
- Panchatcharam BS, Cooksley CM, Ramezanzpour M, Vediappan RS, Bassiouni A, Wormald PJ, Psaltis AJ, Vreugde S. Staphylococcus aureus biofilm exoproteins are cytotoxic to human nasal epithelial barrier in chronic rhinosinusitis. *Int Forum Allergy Rhinol.* 2020;10(7):871–883.